Tree organization method for structuring cluster space-based rover formations with applications to multi-object transportation

Mauro Baquero-Suárez, Ignacio Mas, and Juan Giribet

Abstract In this work, concepts of cluster space approach are extended through a novel formulation, namely Tree Organization Method (TOM), to systematically arrange formations of mobile robots. TOM consists in analyzing the n-robot cluster as an open kinematic chain with multiple branches, where robots remain linked as they move according to this virtual mechanism, by ensuring the specified formation's geometry during all the navigation time. TOM allows to easily generate synchronized reference trajectories for all robots involved in the formation, and this formulation is applied to the particular case of an arranged 7-robot cluster tasked to transport 3 spheres along a predefined trajectory. This scenario is recreated in a realistic cooperative simulation interfacing MSC ADAMS and MATLAB, where multi-body dynamic modeling, cluster specification under TOM and robust tracking controllers are developed for this multi-robot application.

Key words: Mobile Robots, Cluster Space, Robust Control, Multi-body Dynamics.

1 Introduction

Broad communities have been attracted by mobile robotics due to the wide range of recent developed applications around automated navigation tasks where operating conditions or the environments may not be suitable for human execution. Within these applications, those cited in [3, 7] stand out, where mobile robots are used in

✉ Mauro Baquero-Suárez
Instituto Tecnológico de Buenos Aires (ITBA), Departamento de Investigación y Doctorado, Buenos Aires, Argentina. e-mail: `mbaquero@itba.edu.ar`
Ignacio Mas, Instituto Tecnológico de Buenos Aires (ITBA) and CONICET, Argentina. e-mail: `imas@itba.edu.ar`
Juan Giribet, Departamento de Ingeniería Electrónica - Universidad de Buenos Aires and Instituto Argentino de Matemática "Alberto Calderón" (IAM) CONICET, Buenos Aires, Argentina. e-mail: `jgiribet@fi.uba.ar`

navigation-based map-learning tasks, as well as the research on cooperative tasks using multi-robot systems in [2,9] as they adduce several advantages in the formations of synchronized mobile robots, such as flexible reconfigurability, increased coverage, and diverse functionality.

That said, the main objective of this research is the synchronized movement of several specified formations, and the chosen way for achieving it is through the cluster space methodology devised in [4, 6], where desired trajectories are defined within a kinematic representation that involves various centralized attributes as position, orientation, and geometry, by considering the n-robot system as a single entity. This work also enlarges the concept of cluster space by stating a tree organization method (TOM) that allows a suitable addition of members to expand a predefined basic minimal cluster, by means of ramifications that depend on the kinematic behavior of linked anterior robots, such as n-link serial mechanisms. Utility of TOM is demonstrated in this work through a navigation simulation with the 7-robot cluster, where the simultaneous transportation of three spheres (as shown in Fig. 1(c)) is implemented and the correct generation of trajectories is verified.

Then, generated formation reference trajectories are translated to the space of each robot, where whichever tracking controller can be designed to ensure robust tracking. Therefore, the designed tracking controller (TC) in [8] is replicated here to govern the dynamics of each non-holonomic vehicle. This TC is a non-linear feedback structure that uses Lyapunov redesign to ensure robust tracking and rejection of associated side slipping disturbances to the kinematic model. Effectiveness of TC is validated by successful results in a realistic simulation with the virtual dynamic model of a 7-robot cluster developed on MSC ADAMS. ADAMS is a complete modeling software, with potential capabilities to give convincing solutions around simulation of the dynamical behavior of rigid and/or flexible multi-body systems, where dynamics associated to friction, rolling, and collision are easily included to multi-body systems in motion (see [1]). Besides, ADAMS/View has the capability of communicating with MATLAB/Simulink, allowing both computing packages to be linked to simulate both the replicated TC and the specified cluster space representation with the virtual multi-robot system.

2 Robot modeling

According to the scheme exhibited in Fig. 1(a), the kinematic model of an idealized differential-drive wheeled vehicle is

$$\begin{bmatrix} \dot{x} \\ \dot{y} \\ \dot{\theta} \end{bmatrix} = \begin{bmatrix} -\sin\theta & 0 \\ \cos\theta & 0 \\ 0 & 1 \end{bmatrix} \begin{bmatrix} u_1 \\ u_2 \end{bmatrix}, \quad \text{with} \quad \begin{bmatrix} u_1 \\ u_2 \end{bmatrix} = \begin{bmatrix} R/2 & R/2 \\ -R/L & R/L \end{bmatrix} \begin{bmatrix} \omega_l \\ \omega_r \end{bmatrix}, \tag{1}$$

where u_1 and u_2 correspond to the robot's linear and angular velocity magnitudes. The robot moves on the floor surface by generating a trajectory p that depends on the linear velocities $v_r = \omega_r R$ and $v_l = \omega_l R$, with ω_r and ω_l as the angular velocities of right and left wheels and R their radius. The additional rear castor wheel serves as a support point-contact, and it is helpful to the robot's weight distribution.

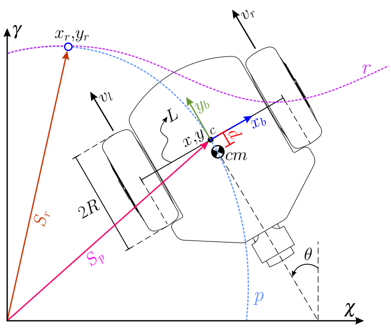

(a) Kinematic model of the mobile robot.

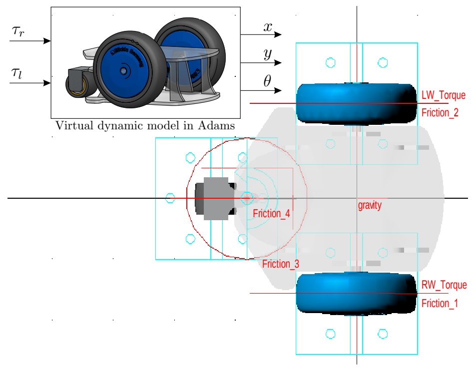

(b) Multi-body dynamic model of the mobile robot.

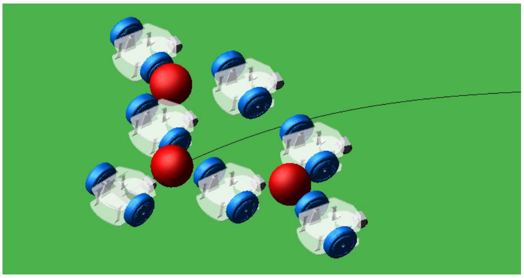

(c) 7-robot cluster transporting three spheres along a path.

Fig. 1 Modeling a two wheeled non-holonomic mobile multi-robot system in MSC ADAMS.

On the other hand, a virtual plant of this vehicle was built on MSC ADAMS by considering the kinematic model in (1) and the physical parameters consigned in Table 1. Fig. 1(b) shows a top view of the virtual robot in ADAMS/View, which is mainly constituted by a chassis, two lateral wheels and a castor wheel mechanism at the rear, and they are connected by revolute joints. Additionally, a flat and rigid surface was created for using it as a road, where contact forces and friction rolling disturbances were modeled. This virtual dynamic model was exported to MATLAB/Simulink as a multiple-input multiple-output (MIMO) non-linear plant, as represented by the block that Fig. 1(b) shows. This connection allowed to develop cooperative simulations where control systems are easily programmed by the simulink's graphical structure to govern the ADAMS model through its input and output variables.

This virtual multi-body system is posteriorly used to build a multi-robot plant with seven vehicles properly accommodated to carry three rigid spheres along the workspace (see Fig. 1(c)). ADAMS simulates several realistic disturbances such as the vibrations and road slips that affect the ideal behavior of each vehicle and

Table 1 Parameters of the mobile robot.

Physical properties of the mobile robot				
Total mass	m_t		1.245 kg	
Radius of the right and left wheels	R		50 mm	
Distance between both lateral wheels	L		156 mm	
Mass moment of inertia of lateral wheels	J		$52.91\ \mathrm{kg \cdot mm^2}$	
Offset distance of center of mass	d		unknown	
Gravity	g		$9.807\ \mathrm{m/s^2}$	
Parameters to model friction into robot's joints				
Parameters		Lateral wheels	Castor wheel	Steering of castor wheel
Static friction coefficient	μ_s	0.15	0.15	0.05
Dynamic friction coefficient	μ_d	0.1	0.1	0.033
Friction arm	R_n	12 mm	6.2 mm	2.5 mm
Pin radius	R_p	8 mm	3.025 mm	2.5 mm
Bending reaction arm	R_b	36 mm	30 mm	3 mm
Stiction transition velocity	v_s	1 mm/s	1 mm/s	1 mm/s
Dynamic transition velocity	v_d	$1.5v_s$	$1.5v_s$	$1.5v_s$
Friction torque preload	T_{pre}	$0.0\ \mathrm{N \cdot mm}$	$0.0\ \mathrm{N \cdot mm}$	$0.0\ \mathrm{N \cdot mm}$
Impact force parameters				
Stiffness			10 N/mm	
Force exponent			2.2	
Damping			$0.2\ \mathrm{N \cdot sec/mm}$	
Penetration depth			1×10^{-3} mm	
Coulomb friction parameters				
Static friction coefficient	μ_{sf}		7.3×10^{-2}	
Dynamic friction coefficient	μ_{df}		5.5×10^{-2}	
Stiction transition velocity	v_{sf}		2 mm/s	
Friction transition velocity	v_{df}		3 mm/s	

sphere in the plant. These disturbances are assumed as unknown dynamics, generated by time-variant contact forces with the road, undesired inertia accelerations and friction torques on wheels' giro axes. Therefore, to deal with these uncertainties, a robust control can be implemented to track a specified set of multi-robot reference trajectories.

3 Multi-robot cluster specification

In order to find a suitable way to distribute and lead a set of modeled mobile robots along an arbitrary trajectory, cluster space approach used in [4, 6] is adopted and extended by the TOM formulation outlined below. Although the proposed methodology is applicable to any multi-robot application, we take here the particular case study of several spheres being simultaneously pushed along a desired trajectory by a group of robots. Under the cluster space flexibility, TOM allows to find a cluster representation for a n-robot system from an already denoted basic k-robot cluster representation ($2 \leq k < n$), with a correct state variables selection for the forward and inverse kinematics. Then, addition of members–where such members can be both robots or clusters–to the basic formation can be done by considering the desired cluster as an open kinematic chain with virtual links, where the behavior of any defined frame in the formation (along $\{\chi, \gamma\}$) depends on the behavior of its predecessor, and previously specified cluster attributes guarantees a global synchronized movement without undesired dynamics such as collisions.

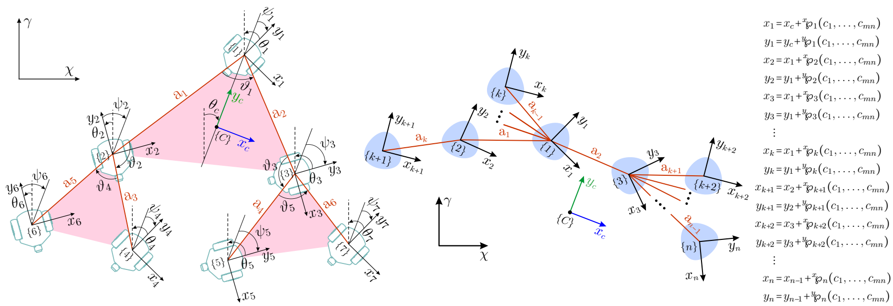

(a) Formation of seven mobile robots. (b) TOM-based formation.

Fig. 2 Analyzed formations under cluster space approach and TOM formulation.

Exhibited scheme in Fig. 2(b) is essentially constituted by ramifications of virtual articulated open chains that satisfy the kinematics of a planar serial robot, which can independently or synchronously be moved with respect to the defined cluster base in the formation. This configuration can cover multiple areas within the workspace, while whichever time-variant geometrical shape required by the navigation task is simultaneously ensured. In general, desired TOM-based cluster attributes according to Fig. 2(b) can be defined by a set of state variables c_i, arranged into a state vector $\mathbf{c} \in \mathbb{R}^{mn}$ to represent the forward kinematics of the n-robot system as follows[1]:

$$\mathbf{c} = \begin{bmatrix} c_1 \\ c_2 \\ \vdots \\ c_{mk} \\ \hline c_{mk+1} \\ \vdots \\ c_{mn} \end{bmatrix} = \begin{bmatrix} f_1(x_1, y_1, \theta_1, \ldots, x_n, y_n, \theta_n) \\ f_2(x_1, y_1, \theta_1, \ldots, x_n, y_n, \theta_n) \\ \vdots \\ f_{mk}(x_1, y_1, \theta_1, \ldots, x_n, y_n, \theta_n) \\ \hline f_{mk+1}(x_1, y_1, \theta_1, \ldots, x_n, y_n, \theta_n) \\ \vdots \\ f_{mn}(x_1, y_1, \theta_1, \ldots, x_n, y_n, \theta_n) \end{bmatrix} \begin{matrix} \left.\begin{matrix} \\ \\ \\ \\ \end{matrix}\right\} k\text{-robot cluster base} \\ \\ \\ \\ \end{matrix} . \quad (2)$$

Then, a set of equations q_i, arranged into a state vector $\mathbf{q} = [x_1, y_1, \theta_1, \ldots, x_n, y_n, \theta_n]^{\mathrm{T}} \in \mathbb{R}^{mn}$ can be similarly established to represent the inverse kinematics of the n-robot system as follows:

$$\mathbf{q} = \begin{bmatrix} q_1 \\ q_2 \\ \vdots \\ q_{mk} \\ \hline q_{mk+1} \\ \vdots \\ q_{mn} \end{bmatrix} = \begin{bmatrix} g_1(c_1, c_2, \ldots, c_{mn}) \\ g_2(c_1, c_2, \ldots, c_{mn}) \\ \vdots \\ g_{mk}(c_1, c_2, \ldots, c_{mn}) \\ \hline g_{mk+1}(c_1, c_2, \ldots, c_{mn}) \\ \vdots \\ g_{mn}(c_1, c_2, \ldots, c_{mn}) \end{bmatrix} \begin{matrix} \left.\begin{matrix} \\ \\ \\ \\ \end{matrix}\right\} k\text{-robot cluster base} \\ \\ \\ \\ \end{matrix} , \quad (3)$$

[1] m corresponds to the degrees of freedom of each robot in the formation.

where computed equations from g_{mk+1} to g_{mn} always will be represented by two components (see equations of Fig. 2(b)). The first component $g(q_{i-j})$ is referred to the movement of the anterior linked robot, while the second component ($\wp_i$) corresponds to its kinematic behavior as a function of the cluster state variables. This approach considerably facilitates the analysis of an arbitrary formation and the calculation of reference trajectories. Furthermore, it differs from other techniques such as the leader-follower scheme outlined in [5], since our method allows the addition of members to the formation as virtual branches, taking into account its shape and geometry with respect to a specific cluster moving frame $\{C\}$, instead of the given approach to the previously cited leader-follower method, where angles and distances between robots are specified with respect to the inertial frame.

According to the proposed methodology and the presented case study, a set of state variables must be selected to capture the forward kinematics of the TOM-based 7-robot cluster illustrated in Fig. 2(a). Firstly, a basic 3-robot cluster space vector $\mathbf{c}_1$ is defined as

$$\mathbf{c}_1 = \left[x_c \; y_c \; \theta_c \; \mathrm{a}_1 \; \mathrm{a}_2 \; \vartheta_1 \; \psi_1 \; \psi_2 \; \psi_3 \right]^{\mathrm{T}}, \tag{4}$$

with

$$x_c = (x_1{+}x_2{+}x_3)/3, \;\; y_c = (y_1{+}y_2{+}y_3)/3, \;\; \theta_c = \mathrm{atan2}\left(x_1{-}x_c, y_1{-}y_c\right), \tag{5}$$

$$\mathrm{a}_1 = \sqrt{(x_1{-}x_2)^2{+}(y_1{-}y_2)^2}, \;\; \mathrm{a}_2 = \sqrt{(x_1{-}x_3)^2{+}(y_1{-}y_3)^2}, \;\; \psi_1 = \theta_1{+}\theta_c, \tag{6}$$

$$\psi_2 = \theta_2{+}\theta_c, \quad \psi_3 = \theta_3{+}\theta_c, \;\; \vartheta_1 = \mathrm{acos}\left[\frac{\mathrm{a}_1^2{+}\mathrm{a}_2^2{-}(x_3{-}x_2)^2{-}(y_3 - y_2)^2}{2\mathrm{a}_1\mathrm{a}_2}\right]. \tag{7}$$

The frame indicating the cluster position $\{C\}$ has been conveniently located at the triangle's centroid of robots $\{1\}$, $\{2\}$, and $\{3\}$, and oriented with x_c pointing towards robot $\{1\}$[2]. Correspondingly, the inverse kinematics of 3-robot cluster is represented by

$$\mathbf{q}_1 = \left[x_1 \; y_1 \; \theta_1 \; x_2 \; y_2 \; \theta_2 \; x_3 \; y_3 \; \theta_3 \right]^{\mathrm{T}}, \tag{8}$$

with

$$x_1 = x_c{+}(\ell \sin\theta_c)/3, \;\; y_1 = y_c + (\ell \cos\theta_c)/3, \;\; \theta_1 = \psi_1{-}\theta_c, \tag{9}$$

$$x_2 = x_1{-}\mathrm{a}_1 \sin\left(\vartheta_1/2{+}\theta_c\right), \;\; y_2 = y_1{-}\mathrm{a}_1 \cos\left(\vartheta_1/2{+}\theta_c\right), \;\; \theta_2 = \psi_2{-}\theta_c, \tag{10}$$

$$x_3 = x_1{+}\mathrm{a}_2 \sin\left(\vartheta_1/2{-}\theta_c\right), \;\; y_3 = y_1{-}\mathrm{a}_2 \cos\left(\vartheta_1/2{-}\theta_c\right), \;\; \theta_3 = \psi_3{-}\theta_c, \tag{11}$$

where $\ell = \sqrt{\mathrm{a}_1^2{+}\mathrm{a}_2^2{+}2\mathrm{a}_1\mathrm{a}_2\cos\vartheta_1}$ (see [4]). Then, four members are added to the 3-robot system to define the 7-robot cluster space vector $\mathbf{c}_2$ as

$$\mathbf{c}_2 = \left[\mathbf{c}_1^{\mathrm{T}} \; \mathrm{a}_3 \; \mathrm{a}_4 \; \mathrm{a}_5 \; \mathrm{a}_6 \; \vartheta_2 \; \vartheta_3 \; \vartheta_4 \; \vartheta_5 \; \psi_4 \; \psi_5 \; \psi_6 \; \psi_7 \right]^{\mathrm{T}}, \tag{12}$$

[2] Two constrains were considered in this 3-robot cluster specification: first, $\mathrm{a}_1{=}\mathrm{a}_2$ to simplify the set of equations into vector field $\mathbf{q}_1$; and second, $0 < \vartheta_1 < \pi$, $0 < \gamma < \{\mathrm{a}_1, \mathrm{a}_2\} < \infty$ to remain a triangle-shape formation between robots without collisions nor singular configurations.

with

$$a_3 = \sqrt{(x_4-x_2)^2+(y_4-y_2)^2}, \ \vartheta_2 = \mathrm{acos}\left[\frac{a_1^2+a_3^2-(x_1-x_4)^2-(y_1-y_4)^2}{2a_1a_3}\right], \tag{13}$$

$$a_4 = \sqrt{(x_3-x_5)^2+(y_3-y_5)^2}, \ \vartheta_3 = \mathrm{acos}\left[\frac{a_2^2+a_4^2-(x_5-x_1)^2-(y_5-y_1)^2}{2a_2a_4}\right], \tag{14}$$

$$a_5 = \sqrt{(x_6-x_2)^2+(y_6-y_2)^2}, \ \vartheta_4 = \mathrm{acos}\left[\frac{a_3^2+a_5^2-(x_4-x_6)^2-(y_4-y_6)^2}{2a_3a_5}\right], \tag{15}$$

$$a_6 = \sqrt{(x_3-x_7)^2+(y_3-y_7)^2}, \ \vartheta_5 = \mathrm{acos}\left[\frac{a_4^2+a_6^2-(x_7-x_5)^2-(y_7-y_5)^2}{2a_4a_6}\right], \tag{16}$$

$$\psi_4 = \theta_4+\theta_c, \ \psi_5 = \theta_5+\theta_c, \ \psi_6 = \theta_6+\theta_c, \ \psi_7 = \theta_7+\theta_c. \tag{17}$$

Then, 7-robot space vector $\mathbf{q}_2$ (or inverse kinematics) results as follows:

$$\mathbf{q}_2 = \left[\,\mathbf{q}_1^{\mathrm{T}} \ x_4 \ y_4 \ \theta_4 \ x_5 \ y_5 \ \theta_5 \ x_6 \ y_6 \ \theta_6 \ x_7 \ y_7 \ \theta_7\,\right]^{\mathrm{T}}, \tag{18}$$

with

$$x_4 = x_2+a_3\sin(\vartheta_1/2+\vartheta_2+\theta_c), \ y_4 = y_2+a_3\cos(\vartheta_1/2+\vartheta_2+\theta_c), \tag{19}$$

$$x_5 = x_3-a_4\sin(\vartheta_1/2+\vartheta_3-\theta_c), \ y_5 = y_3+a_4\cos(\vartheta_1/2+\vartheta_3-\theta_c), \tag{20}$$

$$x_6 = x_2+a_5\sin(\vartheta_1/2+\vartheta_2+\vartheta_4+\theta_c), \ y_6 = y_2+a_5\cos(\vartheta_1/2+\vartheta_2+\vartheta_4+\theta_c), \tag{21}$$

$$x_7 = x_3-a_6\sin(\vartheta_1/2+\vartheta_3+\vartheta_5-\theta_c), \ y_7 = y_3+a_6\cos(\vartheta_1/2+\vartheta_3+\vartheta_5-\theta_c), \tag{22}$$

$$\theta_4 = \psi_4-\theta_c, \ \theta_5 = \psi_5-\theta_c, \ \theta_6 = \psi_6-\theta_c, \ \theta_7 = \psi_7-\theta_c. \tag{23}$$

ϑ_z for $z = 1, \ldots, 5$ are angles with the aim of characterizing the triangle-shapes between robots of the cluster, for this reason, they were constrained as $0 < \vartheta_z < \pi$. 0 and/or π values become the triangles in line segments and this case has been considered as not valid in this application. Neither negative values have been considered as a valid attribute, then, $\vartheta_z = \mathrm{acos}(\ldots)$ satisfy the formulated multi-robot kinematics.

On the other hand, by differentiating $\mathbf{c}_i$, a jacobian matrix $\mathbf{J}_i$ can be developed to map robot velocities to cluster velocities in the form of a time-varying linear function. Then, inverse $\mathbf{J}_i^{-1}$ is used to generate the reference trajectories of each mobile robot, where independent TC are available to track them. In this work, the cluster reference trajectories were defined so that global movements of the 7-robot cluster are kept away from singular configurations of $\mathbf{J}_i^{-1}$, furthermore, asymptotic stability of tracking errors provided by TC ensures that such condition is met.

Additionally, the tracking of these trajectories was achieved in this work by replicating the proposed Lyapunov redesign-based non-linear controller in [8], which is not outlined here due to limited space of this paper. Selected TC is constituted by two control loops in cascade, where inner controller allows a robust angular velocity regulation on the lateral wheels of each robot, while the related disturbances to their giro axes and rolling dynamics are rejected. Then, outer controller establishes a robust tracking of reference trajectories by correcting undesired displacements that slipping disturbances cause on the workspace. That said, this scheme ensures robust tracking, by providing the needed torque input to the motor axes of each robot's lateral wheels (τ_r, τ_l), with a high performance to guarantee the rejection of associated disturbances to the motion and the reaction forces produced by the interaction with the carried spheres[3].

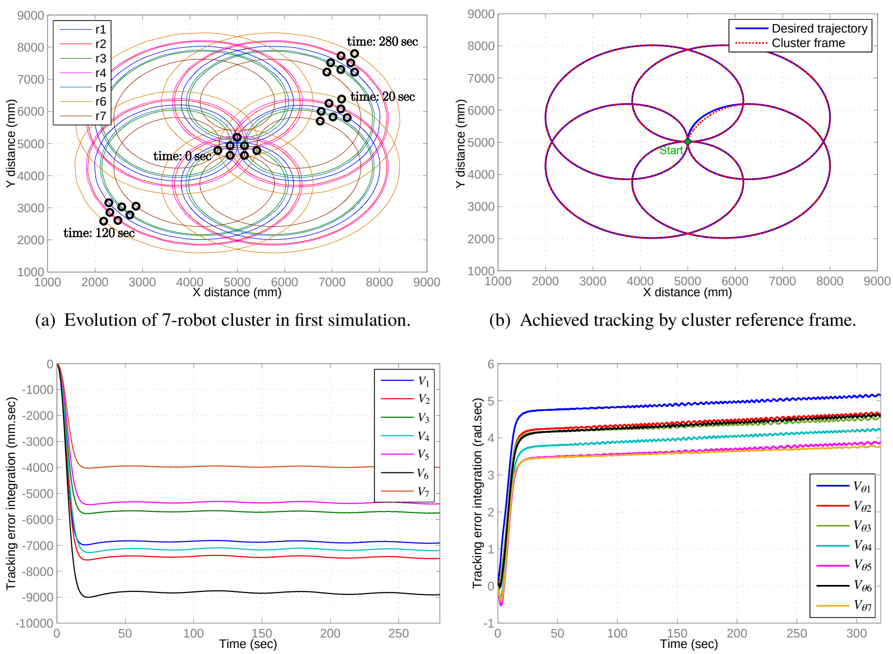

(a) Evolution of 7-robot cluster in first simulation.

(b) Achieved tracking by cluster reference frame.

(c) Evolution of distance functionals.

(d) Evolution of orientation functionals.

Fig. 3 Controlled traveling No. 1 for the 7-robot cluster. Black circles correspond to robots in the formation.

4 Results

Now, taking into account the cluster specifications in Section 3, two dynamic simulations (integrating ADAMS with MATLAB) are presented below to show successful results in the generation and tracking of reference trajectories for the 7-robot cluster of Fig. 2(a), by ensuring the carry of three spheres throughout all time. In the first simulation, the cluster is commanded to track the reference trajectory described by

[3] Given that analyzed mobile robot has a "simple" structure with easily measurable parameters, then, parametric uncertainties have not been contemplated in the control system design and cluster specification.

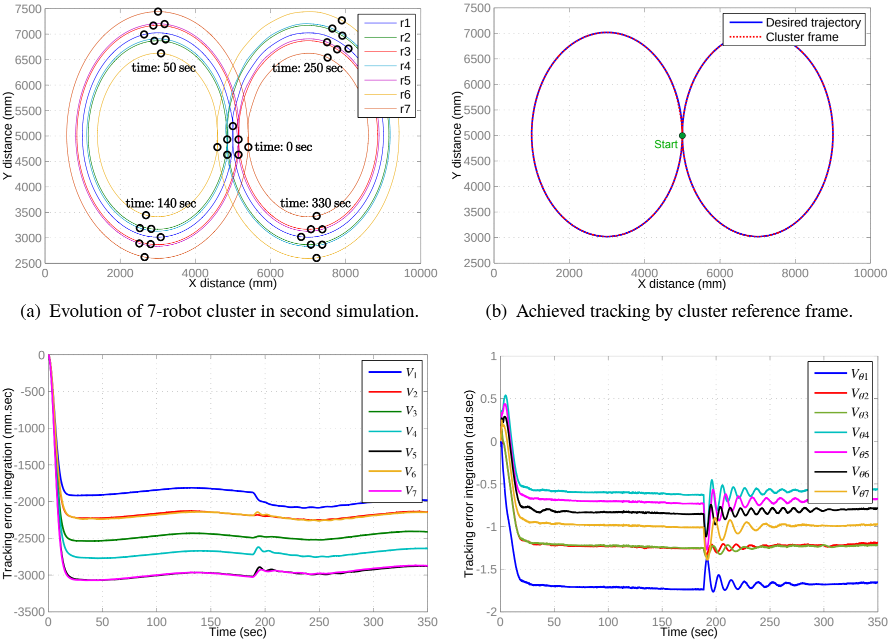

(a) Evolution of 7-robot cluster in second simulation.

(b) Achieved tracking by cluster reference frame.

(c) Evolution of distance functionals.

(d) Evolution of orientation functionals.

Fig. 4 Controlled traveling No. 2 for the 7-robot cluster. Black circles correspond to robots in the formation.

$$\begin{aligned} \dot{x}_c^* &= 6609\left[\cos\left(t/25\right)\sin\left(3t/50\right) + (3/2)\sin\left(t/25\right)\cos\left(3t/50\right)\right]/50 \text{ mm/s}, \\ \dot{y}_c^* &= 6609\left[\cos\left(t/25\right)\cos\left(3t/50\right) - (3/2)\sin\left(t/25\right)\sin\left(3t/50\right)\right]/50 \text{ mm/s}, \end{aligned} \tag{24}$$

with $\left\{x_c^*(0), y_c^*(0)\right\} = \{5000, 5000\}$ mm. Thus, an adequate tracking of TOM-based reference trajectories is achieved by the robots and the cluster moving frame, and it can be appreciated in Fig. 3(a) and Fig. 3(b). Similarly, successful results are also shown in Fig. 4(a) and Fig. 4(b), where the cluster moves through a "∞" shape trajectory that is characterized by

$$\begin{aligned} \dot{x}_c^* &= -2000\left[\sin\left(t/30\right)\right]\left[\text{sign}\left(\sin(t/60)\right)\right]/30 \text{ mm/s}, \\ \dot{y}_c^* &= 2000\left[\cos\left(t/30\right)\right]/30 \text{ mm/s}, \end{aligned} \tag{25}$$

with $\left\{x_c^*(0), y_c^*(0)\right\} = \{5000, 5019\}$ mm. In both simulations, $\vartheta_1, \ldots, \vartheta_5$ and $\mathrm{a}_1, \ldots, \mathrm{a}_6$ remain as time-invariant parameters to encapsulate the three carried spheres[4] within triangular robot formations along the travelled path[5] as shown in Fig. 1(c). Regarding control system performance, tracking error functionals

[4] Carried spheres were modeled as rigid bodies with a diameter of 20 mm, and a weight of 0.18 kg.

[5] Additionally, several simulations for TOM-based multi-robot systems can be found in the following link: `https://youtu.be/ZDyoEHdi27E`.

$$V_i = \int_0^t \left[\left(x_i - x_i^* \right) + \left(y_i - y_i^* \right) \right] dt \text{ and } V_{\theta i} = \int_0^t \left(\theta_i - \theta_i^* \right) dt \tag{26}$$

are respectively exhibited in each simulation (Fig. 3(c)-Fig. 3(d) and Fig. 4(c)-Fig. 4(d)). Under ideal conditions, a constant value trend is expected in computed functionals, however, collisions with the spheres, friction, slip disturbances and other unconsidered dynamics cause the undesired oscillatory behavior shown after 30 seconds, when tracking errors are minimum.

5 Conclusions

Synchronized navigation of multi-robot systems under TOM-based cluster space approach facilitates the construction of references for each member of the stipulated formation while defining shape constraints that simplify the specification of tasks. A case study carrying spheres along a trajectory in a ADAMS/MATLAB simulation showed the effectiveness of the proposed method.

References

1. Baquero-Suárez, M., Cortes-Romero, J., Arcos-Legarda, J., Coral-Enriquez, H.: Estabilización Automática de una Bicicleta sin Conductor mediante el Enfoque de Control por Rechazo Activo de Perturbaciones. Revista Iberoamericana de Automática e Informática industrial **15**(1), 86–100 (2017). DOI 10.4995/riai.2017.8832
2. Ding, L., Gao, H., Deng, Z., Li, Y., Liu, G., Yang, H., Yu, H.: Three-layer intelligence of planetary exploration wheeled mobile robots: Robint, virtint, and humint. Science China Technological Sciences **58**(8), 1299–1317 (2015). DOI 10.1007/s11431-015-5853-9
3. Filliat, D., Meyer, J.A.: Map-based navigation in mobile robots:: I. a review of localization strategies. Cognitive Systems Research **4**(4), 243–282 (2003). DOI https://doi.org/10.1016/S1389-0417(03)00008-1
4. Kitts, C.A., Mas, I.: Cluster space specification and control of mobile multirobot systems. IEEE/ASME Transactions on Mechatronics **14**(2), 207–218 (2009). DOI 10.1109/TMECH.2009.2013943
5. Mariottini, G.L., Morbidi, F., Prattichizzo, D., Vander Valk, N., Michael, N., Pappas, G., Daniilidis, K.: Vision-based localization for leader–follower formation control. IEEE Transactions on Robotics **25**(5), 1431–1438 (2009). DOI 10.1109/TRO.2009.2032975
6. Mas, I., Kitts, C.A.: Dynamic control of mobile multirobot systems: The cluster space formulation. IEEE Access **2**, 558–570 (2014). DOI 10.1109/ACCESS.2014.2325742
7. Meyer, J.A., Filliat, D.: Map-based navigation in mobile robots:: Ii. a review of map-learning and path-planning strategies. Cognitive Systems Research **4**(4), 283–317 (2003). DOI https://doi.org/10.1016/S1389-0417(03)00007-X
8. Shafiei, M., Monfared, F.: Design of a Robust Tracking Controller for a Nonholonomic Mobile Robot with Side Slipping based on Lyapunov Redesign and Nonlinear H∞ Methods. Systems Science & Control Engineering **7**(1), 1–11 (2019). DOI 10.1080/21642583.2018.1555061
9. Villa, D.K.D., Brandão, A.S., Sarcinelli-Filho, M.: A survey on load transportation using multirotor UAVs. Journal of Intelligent & Robotic Systems (2019). DOI 10.1007/s10846-019-01088-w